Supporting Information

Mechanically Self-assembled, Three-dimensional Graphene-Gold Hybrid Nanostructures for Advanced Nanoplasmonic Sensors

Juyoung Leem [†], Michael Cai Wang [†], Pilgyu Kang [†], and SungWoo Nam [, †, §]*

[†]Department of Mechanical Science and Engineering, University of Illinois at Urbana-Champaign, IL, 61801.

[§]Department of Materials Science and Engineering, University of Illinois at Urbana-Champaign, IL, 61801.

** Corresponding Author: swnam@illinois.edu*

METHODS

Graphene-gold nanoparticle hybrid structure fabrication

Graphene was synthesized on a 25 μm thick copper (Cu) foil (Alfa Aesar, MA) by chemical vapor deposition (CVD) system (Rocky Mountain Vacuum Tech Inc., CO). The chamber temperature was raised to 1050 °C under hydrogen (H_2) environment at 150 mTorr. The annealing process was followed at 1050 °C for 35 minutes. Then methane (CH_4) gas was introduced into the chamber at 520 mTorr for 2 minutes for graphene synthesis. Finally the chamber was cooled down slowly while fast cooling was applied to the Cu foil under Argon (Ar) environment. After the synthesis, unwanted graphene flakes at the bottom side of the Cu foil were removed by oxygen plasma etching (Diener GmbH, Germany).

A thin film of gold (Au) was deposited onto graphene on a Cu foil by a thermal evaporator (Nano 36, Kurt J. Lesker, PA) at a deposition rate of 0.1 Å/s in high vacuum ($\leq 5\times10^{-6}$ Torr). The Au film on graphene/Cu foil substrate was then annealed at an elevated temperature (150, 200, 250, 300, 400, and 500 °C) to form Au nanoparticles (NPs) from the Au film under Ar environment with a pressure of 330 mTorr.

Graphene-Au NPs hybrid structure was transferred from a Cu foil to a polystyrene (PS) substrate (K&B Innovations, WI) by wet-transfer. The Au NPs on a graphene/Cu substrate was carefully floated onto sodium persulphate ($Na_2S_2O_8$) (Sigma Aldrich, MA) aqueous solution to etch away the Cu foil (~1 hour). After Cu was completely dissolved in the etchant solution, the graphene-Au NPs film was then transferred onto a surface of deionized (DI) water for cleaning by using a slide glass. Finally, the film was transferred onto a PS substrate.

Au NPs/graphene on a PS sheet was then thermally treated to be shrunken in a laboratory oven (BINDER, Germany) at 110 °C for 1 hour. The amount of shrinkage was controlled by controlling the heating temperature and time.

Structural analysis

Scanning electron microscope (SEM) (S-4800, Hitachi, Japan) images were used for particle analysis. Au NPs were formed on graphene under 22 different combinations of Au deposition thicknesses (0.1, 0.5, 1.0, 1.5, 2.0, 3.0, and 4.0 nm) and dewetting temperatures (150, 200, 250, 300, 400, and 500 °C).

Particle size and gap distance analysis were performed using ImageJ.[1] SEM images for selected cases were cropped into 500 nm by 500 nm regions for image analysis. A total of ~600 NPs were analyzed from five to seven images for each case for the analysis results presented in Figure S4.

Optical microscope images shown in Figure 2c and 2d were captured using an optical microscope in reflection dark-field mode (Axio Imager M2m, Carl Zeiss, Germany). Top view SEM images in Figure 2e and 2f were obtained as-is (without application of any conductive coating layer), and side view SEM images in Figure 2g and 2h were obtained with a 5 nm thick AuPd coating to prevent electron charging from the PS substrate during SEM imaging (S-4800, Hitachi, Japan).

SERS measurement

Surface enhance Raman spectroscopy (SERS) data shown in Figure 3 and Figure S8 were obtained with a 633 nm laser at 1800 l/mm grating and 10 seconds accumulation (InVia

microPL, Renishaw, UK). To plot the data, the average intensity of SERS signals from five different points were taken from each case. The averages and standard deviations were calculated based on those measurements. Rhodamine 6G (R6G) (Sigma Aldrich, MA) was selected as a target and dissolved into DI water for measurement. For Figure 3b, 1mM R6G aqueous solution was filled into a wall made of polydimethylsiloxane (PDMS) (SYLGARD-184, Dow Corning, MI) for wet-condition measurement.

SERS data shown in Figure 4a was obtained with a 785 nm laser at 300 l/mm grating and 10 seconds accumulation (LabRAM HR 3D, Horiba, Japan). 4-Mercaptophenol (4-MPH) (Sigma Aldrich, MA) was selected as a target and dissolved into ethanol (200 proof, Decon Labs Inc., PA) to yield different concentration solutions: 1 mM, 100 μM, 10 μM, 1 μM, 100 nM, and 10 nM. Dry-condition measurement was performed with the samples prepared with similar procedures reported earlier by Lee *et al*.[2] First, crumpled graphene-Au NPs substrate was incubated in the solution for 3 hours. Then the substrate was dipped into the pure ethanol and taken out twice for cleaning any excessive 4-MPH molecules. Finally, the substrate was dried overnight.

Electromagnetic simulation

Finite element method (FEM) numerical electromagnetic simulations were conducted using COMSOL Multiphysics software using the RF module. In the simulation, Au NPs were defined as hemispheres with a diameter of 30 nm and graphene was defined with a thickness of 1 nm on a PS substrate. A plane light wave was launched perpendicular to the substrate with single, polarized electric field. As boundary conditions, all outmost sides were defined as perfect matching layer (PML). The refractive index of graphene is governed by $\varepsilon_r(\omega) = 5.5 + i\sigma_0/(\omega\varepsilon_0 d)$

where σ_0 is interband optical conductivity (=$2\pi e^2/4h$, approximately a constant in the visible range), ε_0 is vacuum permittivity (= 8.854 $\times 10^{-12}$ F / m), and d is graphene thickness (= 3.8 Å).[3,4]

Modeling the structural parameters of the crumpled graphene-Au hybrid material

We carried out an estimation of the structural parameters of the crumpled graphene-Au hybrid material using analytical models. Based on its morphology (Figure 2h), and the biaxial strain state, we assumed that the crumpled structure takes on a checkerboard buckling mode.[5] The out-of-plane displacement of checkerboard buckling mode is described by

$$w = A\cos\left(\frac{2\pi x_1}{\lambda_1}\right)\cos\left(\frac{2\pi x_2}{\lambda_2}\right) \tag{1}$$

where w is the crumple profile in the out-of-plane direction, A is the crumple height, and λ_1 and λ_2 are wavelengths along the x_1 and x_2 in-plane directions, respectively. As derived and modeled in ref 5, by minimizing the total energy (i.e., bending energy, membrane energy and strain energy) with respect to the wavelengths and amplitude,[5] the relationships between wavelengths/amplitude and materials properties are expressed as equations (2)-(4):

$$\lambda_1^{-2} + \lambda_2^{-2} = \frac{1}{\left(2\pi \cdot h_f\right)^2}\left(\frac{3\bar{E}_s}{\bar{E}_f}\right)^{2/3} \tag{2}$$

$$\lambda_1^{-2} - \lambda_2^{-2} = \frac{1}{\left(2\pi \cdot h_f\right)^2}\left(\frac{3\bar{E}_s}{\bar{E}_f}\right)^{2/3} \cdot \left(\frac{3-\nu_f}{3+\nu_f}\right) \cdot \left(\frac{\varepsilon_{11}^{pre} - \varepsilon_{22}^{pre}}{\varepsilon_{11}^{pre} + \varepsilon_{22}^{pre} - \left[\left(3\bar{E}_s/\bar{E}_f\right)^{2/3}/2\left(1+\nu_f\right)\right]}\right) \tag{3}$$

$$A = 4h_f \left(\frac{\bar{E}_f}{3\bar{E}_s} \right)^{1/3} \sqrt{\frac{1}{3-\nu_f} \left[\varepsilon_{11}^{pre} + \varepsilon_{22}^{pre} - \frac{(3\bar{E}_s / \bar{E}_f)^{2/3}}{2(1+\nu_f)} \right]} \quad (4)$$

where h_f is the effective film thickness, $\bar{E}_s$ and $\bar{E}_f$ are plane strain moduli of substrate and film respectively, ν_f is Poisson's ratio of the film, and ε_{11}^{pre} and ε_{22}^{pre} are applied strains along x_1 and x_2 directions, respectively. ε_{11}^{pre} and ε_{22}^{pre} are calculated from the change in the linear dimensions of the PS substrate. As shown in Figure 2a and 2b, the substrate was shrunken from a dimension of 10.2 cm by 5.0 cm to a dimension of 5.3 cm by 2.7 cm. The applied strain is defined as equation (5):

$$\varepsilon = \frac{L - L_0}{L_0} \quad (5)$$

where L is the final length and L_0 is the initial length. Since PS is prestrained, ε_{11}^{pre} is calculated to be 0.92 and ε_{22}^{pre} is calculated to be 0.85. The calculated values are close enough to be assumed as $\varepsilon_{11}^{pre} \approx \varepsilon_{22}^{pre} = \varepsilon^{pre}$, and ε^{pre} (=0.89) is defined as the average value of ε_{11}^{pre} and ε_{22}^{pre} in further calculations. This assumption allows equations (2) and (4) to be simplified into equation (6) and (7), respectively:

$$\lambda^{-1} = \frac{1}{2\pi\sqrt{2}} \frac{1}{h_f} \left(\frac{3\bar{E}_s}{\bar{E}_f} \right)^{1/3} \quad (6)$$

$$A = h_f \sqrt{\frac{8}{(3-\nu_f)(1+\nu_f)} \left(\frac{\varepsilon^{pre}}{\varepsilon_{checkerboard}^{c}} - 1 \right)} \quad (7)$$

where $\varepsilon^{c}_{checkerboard} = (3\bar{E}_s / \bar{E}_f)^{2/3} / 4(1+\nu_f)$ is the critical strain that is needed for the checkerboard buckling mode to be initiated. For the calculation, we used 3.34 nm for h_f (effective film thickness, which is the sum of graphene thickness (0.34 nm) and thickness of deposited Au (3.0 nm)), 3.42 GPa[6] and 1 TPa[7] for $\bar{E}_s$ and $\bar{E}_f$, respectively. The calculated values of λ and A are 137.9 nm and 48.8 nm, respectively.

Finally, the aspect ratio (=A/λ) of the crumpled graphene-Au hybrid structure is estimated to be 0.35 when equi-biaxial/uniform shrinkage of ~48% occurs in both x_1 and x_2 directions. The estimated wavelength (137.9 nm) and amplitude (48.8 nm) are smaller than the observed wavelength (~500 nm) and amplitude (~300 nm) from the cross-sectional SEM (Figure S7). The difference between the estimated values and the observed values are likely explainable by our assumptions. In this estimation, we assumed that the contribution of Au NPs to the buckling process is negligible; therefore we used only graphene's Poisson's ratio for ν_f and graphene's plane strain modulus for $\bar{E}_f$. However, Au NPs decorated on graphene may contribute to the shape of the final structure. We note that more precise solid mechanics simulation would be required in order to accurately estimate and model the structural parameters of crumpled graphene-Au hybrid structures.

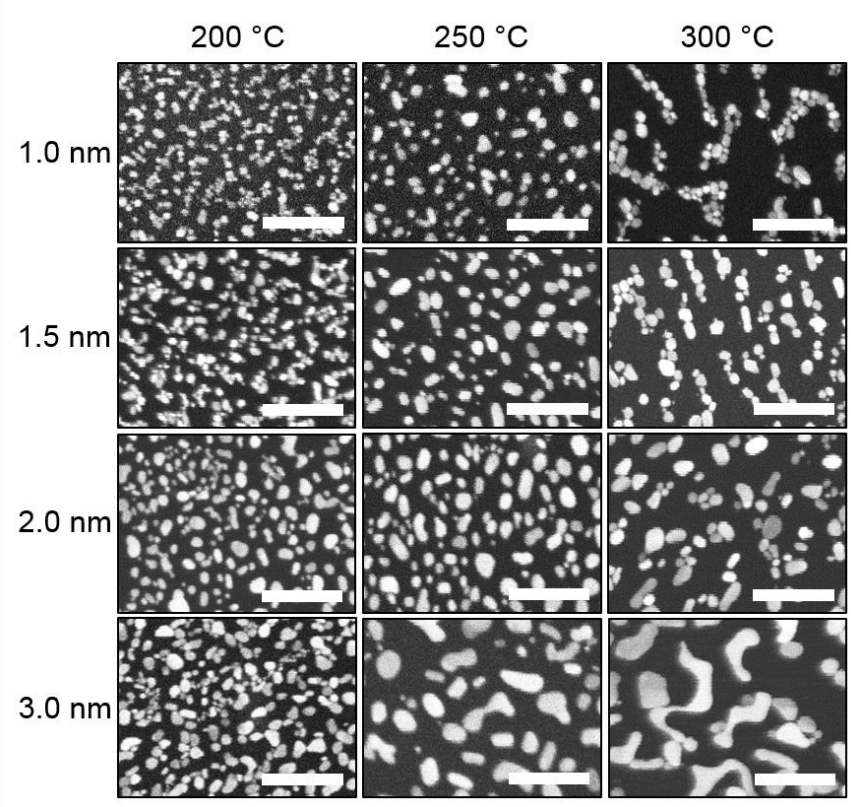

Figure S1. SEM images of 12 different thin film dewetting conditions consisting of four different Au deposition thicknesses and three different dewetting temperatures. Larger particles are obtained with a thicker Au film and a higher dewetting temperature. An upper limit in achievable NP diameter is observed when further increasing the dewetting temperature yields particles that are continuous, elongated shaped structures rather than spherical, as the cases of 3.0 nm Au/300 °C. Scale bars: 250 nm.

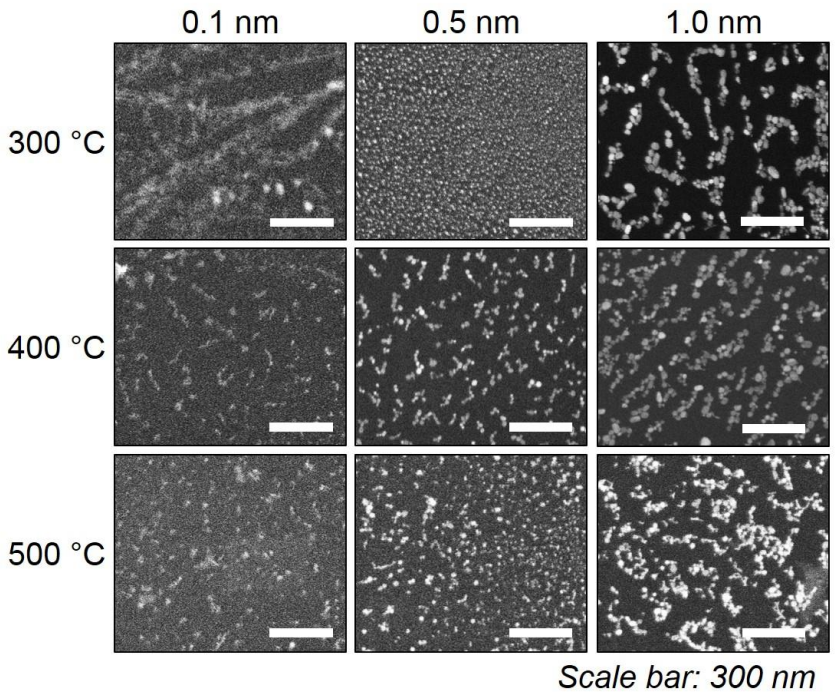

Figure S2. Additional dewetting conditions for Au NP size control. SEM images of nine different cases with three different Au deposition thicknesses (0.1, 0.5, and 1.0 nm) and three different dewetting temperatures (300, 400, and 500 °C). A minimum achievable diameter of generated NPs is difficult to define as the smallest NPs are below the resolution limit of the SEM.

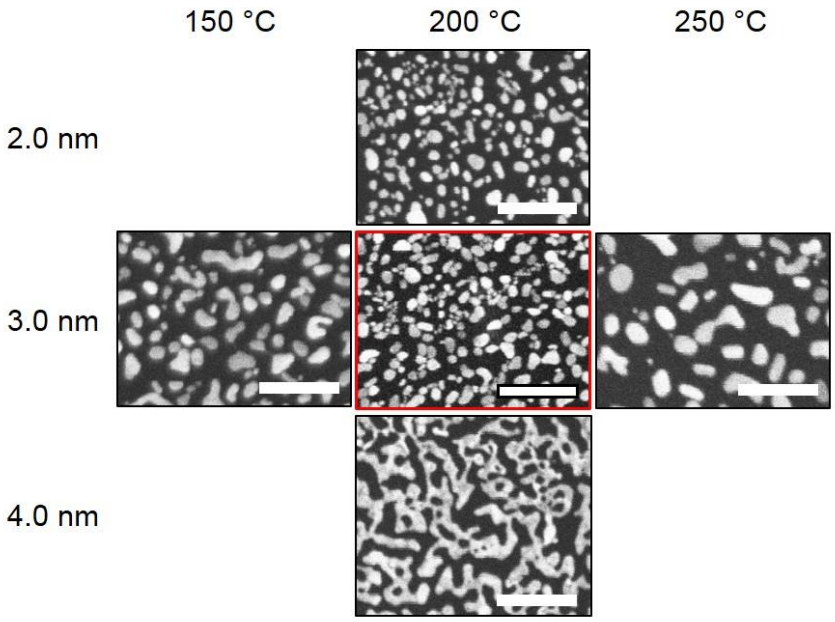

Figure S3. Five selected dewetting conditions in the parameter space adjacent to the optimized condition for Au NP formation (3.0 nm Au and 200 °C dewetting temperature). SEM images show different morphologies formed from higher (250 °C) and lower (150 °C) dewetting temperatures with a fixed Au thickness (3.0 nm, three horizontal panels), and thicker (2.0 nm) and thinner (4.0 nm) Au thickness with a fixed dewetting temperature (200 °C, three vertical panels). 4.0 nm Au/200 °C case shows the upper limit in achievable NP diameter and it generates continuous, elongated shaped structure rather than spherical. Scale bars: 250 nm.

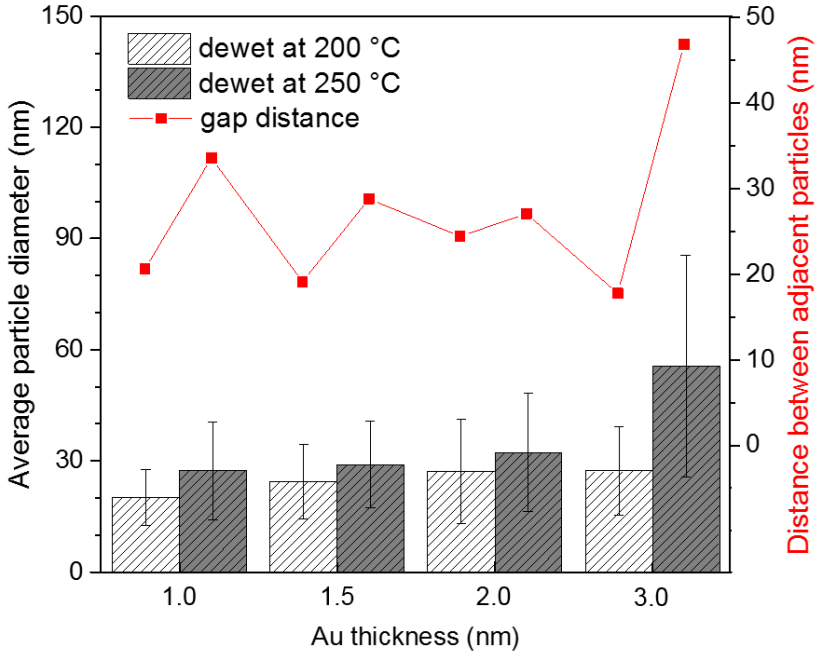

Figure S4. Image analysis of Au NPs sizes and gap distances on flat graphene after dewetting. Bar graph: the average particle diameters and their 1-standard deviations for each case; Line graph: gap distance between adjacent particles based on the data shown in the bar graph.

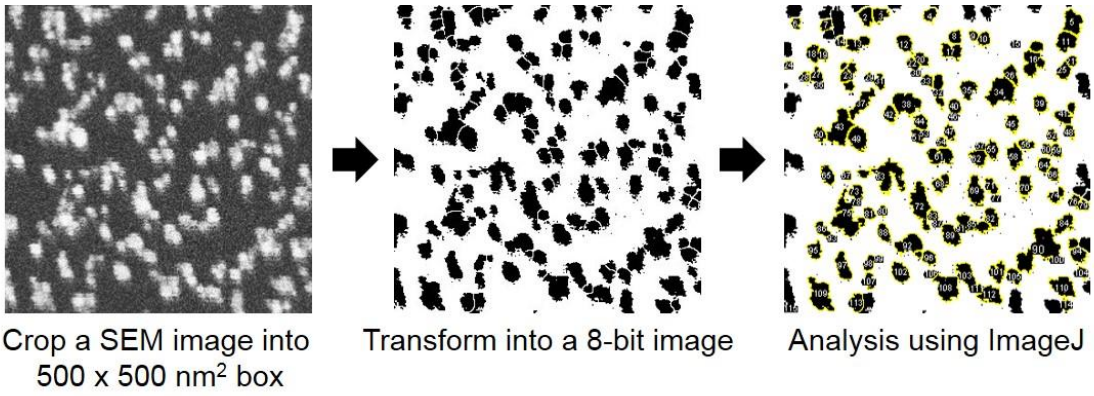

Figure S5. Au NP analysis process. SEM images are cropped 500 nm by 500 nm. Then the images are transformed into 8-bit image. Finally, the area of each particle and number of particles are calculated by ImageJ.

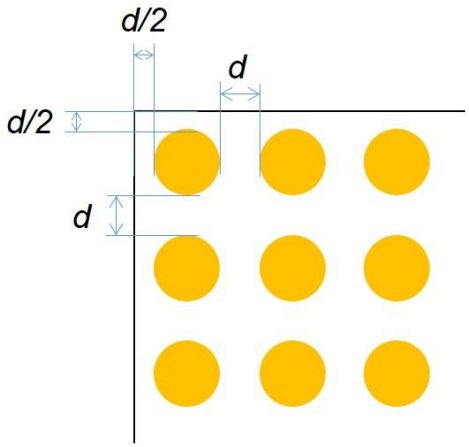

Figure S6. Gap distance calculation. Rectangular particle arrangement was assumed for the gap distance calculation.

Gap distance calculation

Gap distance (*d*) was calculated based on the particle analysis data which is shown in Figure S4 as bar graphs. For simplicity, the arrangement of particles is assumed to be rectangular as shown in Figure S6.

The calculation was performed based on the equation below:

$$d = \frac{\sqrt{N_{images} \times (500 \times 500) nm^2}}{\sqrt{N_{particles}} + 1} - D_{avg}$$

Where d represents distance between adjacent particles, N_{images} represents number of images used for the analysis, $N_{\text{particles}}$ represents number of particles, and D_{avg} represents the average diameter of particles. In addition, (500×500) nm^2 represents the area of each standardized image used for the analysis. N_{images} is a known value; $N_{\text{particles}}$ and D_{avg} are obtained from the individual particle analysis of each image.

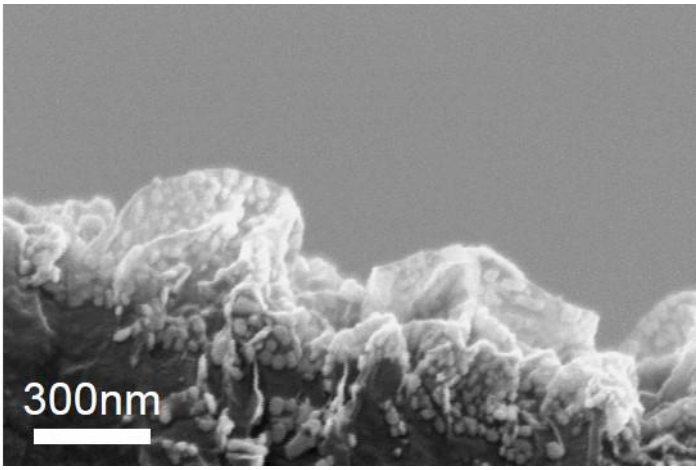

Figure S7. SEM cross sectional view of crumpled graphene-Au NPs hybrid structure. The average height and wavelength of crumpled graphene are estimated to be ~300 nm and ~500 nm, respectively.

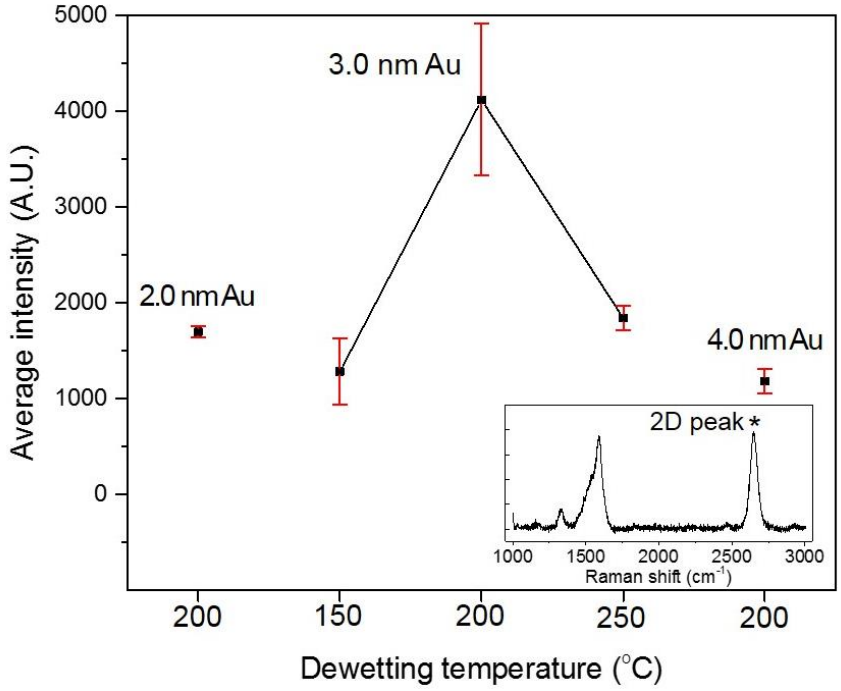

Figure S8 Comparison of Raman enhancement from the cases shown in Figure S3. Graphene 2D peak (at 2650 cm^{-1}) was selected to compare the Raman enhancement due to the Au NPs. Inset: Raman signal of crumpled graphene-Au NPs substrate. Error bars represent 1-standard deviation.

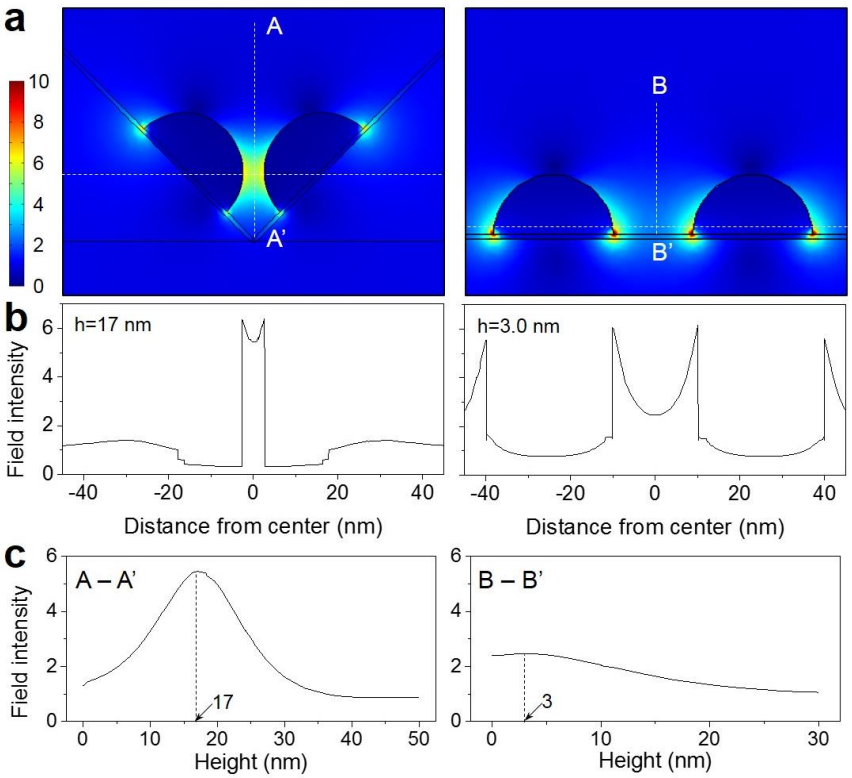

Figure S9. (a) Electromagnetic field enhancement of a crumpled (left) and a flat structure (right) with a 785 nm laser wavelength simulated using COMSOL multiphysics. (b) Line plots of field enhancement are shown across two particles on a crumpled (left) and a flat substrate (right). Those plots are at the heights of 17 nm and 3.0 nm respectively, which are the heights with the highest field enhancement values as shown in (c). (c) Line plots of field enhancement between two particles on a crumpled (left) and a flat substrate (right) with respect to the cross lines A-A' and B-B' in (a) respectively. All values are normalized to the incident field intensity.

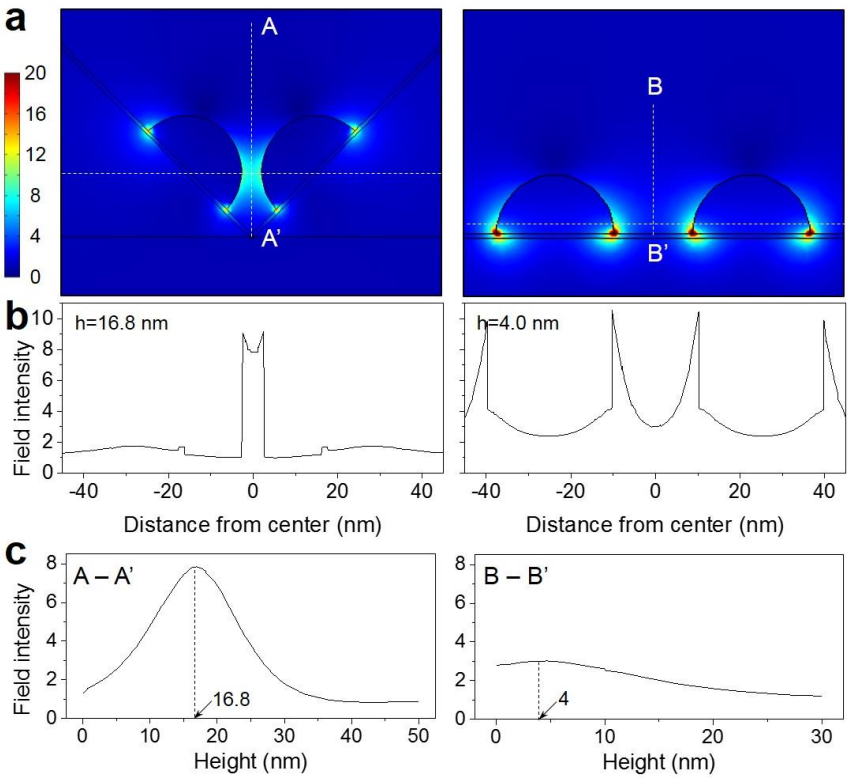

Figure S10. (a) Electromagnetic field enhancement of a crumpled (left) and a flat structure (right) with a 633 nm laser wavelength simulated using COMSOL multiphysics. SERS measurement was performed using a 633 nm laser with R6G solutions (Figure 3b). (b) Line plots of field enhancement are shown across two particles on a crumpled (left) and a flat substrate (right). Those plots are at the heights of 16.8 nm and 4.0 nm respectively, which are the heights with the highest field enhancement values as shown in (c). (c) Line plots of field enhancement between two particles on a crumpled (left) and a flat substrate (right) with respect to the cross lines A-A' and B-B' in (a) respectively. All values are normalized to the incident field intensity.

REFERENCES

(1) Rasband, W.S., ImageJ, U. S. National Institutes of Health, Bethesda, Maryland, USA, http://imagej.nih.gov/ij/, 1997-2014.

(2) Lee, S.; Hahm, M. G.; Vajtai, R.; Hashim, D. P.; Thurakitseree, T.; Chipara, A. C.; Ajayan, P. M.; Hafner, J. H. *Adv. Mater.* **2012**, *24* (38), 5261–5266.

(3) Gray, A.; Balooch, M.; Allegret, S.; De Gendt, S.; Wang, W.-E. *J. Appl. Phys.* **2008**, *104* (5), 053109.

(4) Mak, K. F.; Ju, L.; Wang, F.; Heinz, T. F. *Solid State Commun.* **2012**, *152* (15), 1341–1349.

(5) Song, J.; Jiang, H.; Choi, W. M.; Khang, D. Y.; Huang, Y.; Rogers, J. A. *J. Appl. Phys*. **2008**, *103* (1), 014303.

(6) Mott, P. H.; Dorgan, J. R.; Roland, C. M. *J. Sound Vib.* **2008**. *312*, 572-575.

(7) Zang, J.; Ryu, S.; Pugno, N.; Wang, Q.; Tu, Q.; Buehler, M. J.; Zhao, X. *Nat. Mater*. **2013**, *12* (4), 312-325.